

Analysis, Design and Development of a Non-Contact Charging system for Smartphones

Abdulrahman Ogunji^{1,2}, Adesanya Atilade², Adebayo Salaam², Sunday Ajayi,² Joseph Olakunle Coker²

¹ De Montfort University, Leicester United Kingdom.

² Lagos State Polytechnic, Ikorodu, Lagos, Nigeria.

Email: ogunjiabdulrahman@gmail.com

Abstract

The analysis on design and implementation of a non-contact charging system is carried out for a smart phones application. This design is basically on half-bridge LLC resonant converter that consist of Pulse Width Modulation, gate driver and receiver circuits. TL494 and IR2110 integrated circuits were used for control of the signals as the duty cycle is 50%, the dead time for proper operation, the resonant and switching frequencies was set at 100 kHz respectively. An inductive circuit is being implemented such that the energy is transfer from transmission coil into receiver coil in order to achieve the set objective, voltage achieved are 5 V and 3.1 V before and after load, as the current is 25 mA while the efficiency between the coils was 46 %. There is correlation between the waveforms achieved by the simulated and implemented circuits. This design is considered to be safe, simple, robust and cost efficient as against the conventional charging system which involves the connection of charger to the mains in order to charge smart phones.

Keywords: Gate Driver Integrated Circuit, Non – Contact Charging, Pulse Width Modulation, Receiver, Simulation, Smart Phones, Transmission Coil.

1.0 Introduction

In the recent time advances in smart phones, laptops, camera, I pad and some other low powered electronics appear to be unlimited, there operations which on batteries remains a weakness, due to a limited lifetime with requirement of a fast, constant and reliable charge time to achieve continuous operation [1]. The challenges of classical and conventional (i.e. traditional) charging system facing the users of these low powered electronics devices as called for concern and in finding lasting solution to this problem, a renew interest in the wireless or non-contact charging system will be the solution.

Wireless or Non-contact power transfer is a process that occurs in any system where electrical energy is transmitted from a power source to a load without the connection of electrical conductors. This system is not new, from the time of Ampere and Faraday, the idea of wireless transmission of power has always been that hope to achieve. Hertz works at high frequency where energy from a spark was coupled from a loop to another which leads to modern radio system using today, propagating power over large distances but with low efficiency [2]. Faraday converts direct current to an alternating current in which Nikola Tesla improved on his work and used the principle of electrodynamics' induction to transfer electromagnetic energy without the need of wires to transmit power from one point to another. This non-contact or wireless power transfer found application in using it as a charger refers to as an inductive charging system. Inductive charging works on the principle in which two power systems are placed very

close to one another [3]. This inductive charging system has some advantages which are wireless, charging number of devices at a time, electrically safe, waterproof and low maintenance and disadvantages which are more power consumption, low efficiency, more heat generation, complex circuit and high cost of construction [3].

This work is basically on design of a non-contact charging system for smartphones, which will consist of circuit of a power transmitter attached to the vehicle power supply, a circuit of power receiver attached to a micro-USB plug suitable to connect to the phone and this is capable of charging Smartphones with a certain current at a regulated voltage of 5V. Both the transmitter and receiver are fitted electrical coils in which when both are brought into physical proximity, power flows from the transmitter to the receiver. This non-contact charging system is working on principle of mutual inductance which is categorically called inductive charging system.

2.0 Device Working Principle

The basic Non-contact charging system consists of several modules as shows in figure 1. The architecture which includes direct current source, the converter (i.e. convert direct to alternating current) attached with transmitting coil, rectifier (i.e. convert alternating to direct current) with receiver coil, voltage regulator and load.

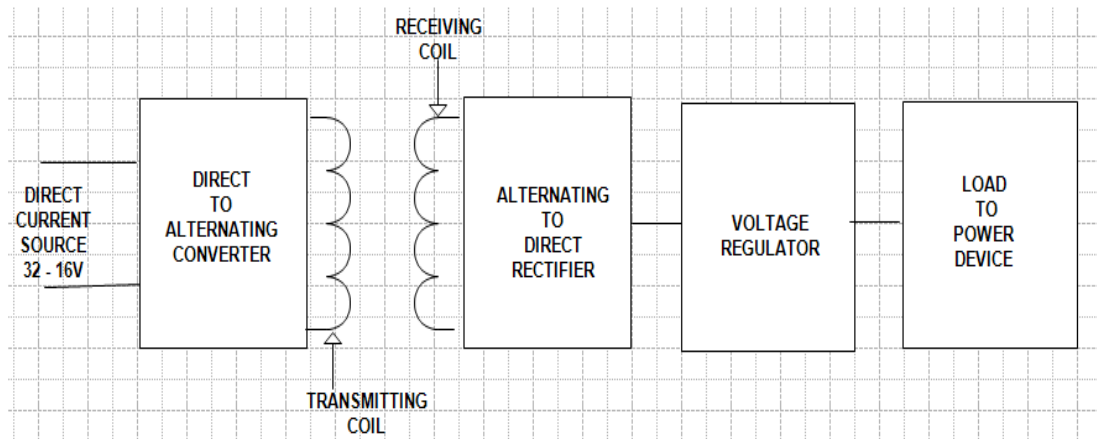


Figure 1: Block diagram of Non-contact charging system

Direct current source ranging between 16 – 32V from the car battery supply to the converter, the converter can be in any form such as inverter, oscillator or any type of converter that can convert direct to alternating current and posses enough power for transmitting coil. On the other side of the module, the receiving coil, which operate at the same frequency with the transmitting coil, receiving a signal from the transmitting side and this is based on the strength and the distance between the transmitter and the receiver, the rectifier convert alternating current from the coil to direct current, the voltage regulator, regulate the output voltage from the rectifier to 5V for the charging of the smart phones. In this work, the LLC resonant converter will be adopted as the converter which can be used for the conversion of direct current from the car battery to alternating current for the transmitting coil. While on the receiver side, the

rectify circuit that consist of four diodes connected in the bridge form such that the two alternating diodes are operating in forward bias and the two remaining diodes will be operating at reverse bias for the positive half cycle. In the negative half cycle, this will operate in alternate mode, for the completion of the other cycle.

3.0 Design Approach

The half-bridge LLC resonant converter design goal is to achieve maximum loss with the capability of achieve required maximum gain to ensure wide operation range. The proposed design for the converter is going to be in sections such that the Pulse with Modulation circuit, gate drive circuit, the resonant circuit and the rectifier circuit will be considered separately and the calculations will be based on an assumed specification for the Non-contact charging system.

3.1 Pulse Width Modulation generation

The generation of analogue signal using a digital source and the method used is called Pulse Width Modulation. There are two components that determine this signal behaviour and they are duty cycle and frequency. The duty cycle describes the amount of time the signal is in ON state as a percentage of the total time of it takes to complete one cycle while frequency determines how fast the PWM complete a cycle and how fast it switches between the ON and OFF states.

In this work, TL494 PWM controller IC is used as a Pulse Width Modulation generator device. This device is a fixed –frequency, pulse width modulation control circuit, incorporating the primary building blocks required for the control of a switching power supply. Furthermore, it consists of two error amplifiers, a pulse-steering flip flop, 5V reference voltage circuit, a PWM comparator, a dead time comparator and an oscillator. Above all, this device has an operating frequency ranging between 1 KHz to 300 KHz [4]

The modulation of output pulse of this device is accomplished by comparing the sawtooth waveform created by the internal oscillator on the timing capacitor (C_T) to either of two control signals. As the control signal increases, the time during which the sawtooth input is greater decreases; therefore, the output pulse duration decreases. A pulse steering flip flop alternately directs the modulated pulse to each of the two output transistors [4]

3.1.1 Design calculation

The approximate oscillator frequency of this device is determined by:

$$f_{osc} = \frac{1.1}{2 \times C_T \times R_T} [4]$$

Where C_T is timing capacitor and R_T is the timing resistor

If 100 KHz is considered as the oscillator frequency, then an actual timing resistor from figure 2 can be determine.

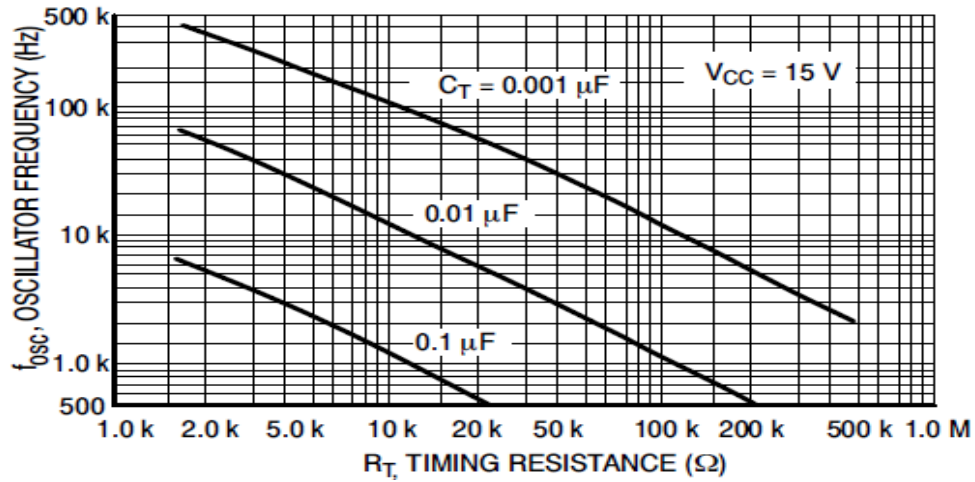


Figure 2: Oscillator frequency – Timing resistance chart

From figure 7, R_T is 20 K Ω , and then timing capacitor is calculated by this expression

$$C_T = \frac{1}{2 \times R_T \times f_{osc}}$$

$$= \frac{1}{2 \times 20 \times 10^3 \times 100 \times 10^3}$$

$$C_T = 0.001\mu F$$

Therefore, timing capacitor for the PWM generator circuit is 0.001 μ F.

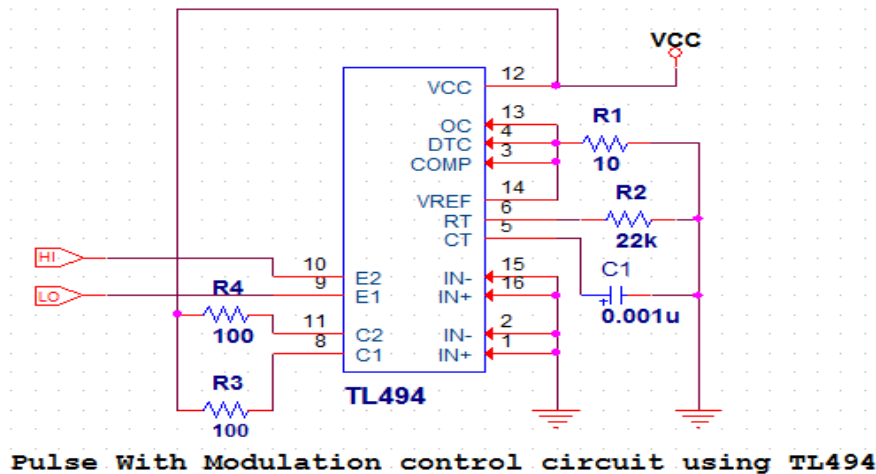


Figure 3: PWM circuit using TL494

3.2 Gate driver circuit

The circuit that generate the frequency signal or Pulse Width Modulation is not capable of driving the switches (i.e. MOSFETS) directly, hence, there is need to have another device most especially an integrated circuit, which can drive the gate of the switches simultaneously. The gate driver is capable of supplying sufficient current and voltage needed to switch the MOSFETS for the power converter operation. This driver is also capable of providing isolation required between the high and low sides of the power converter such that the MOSFETS can work in an alternate form.

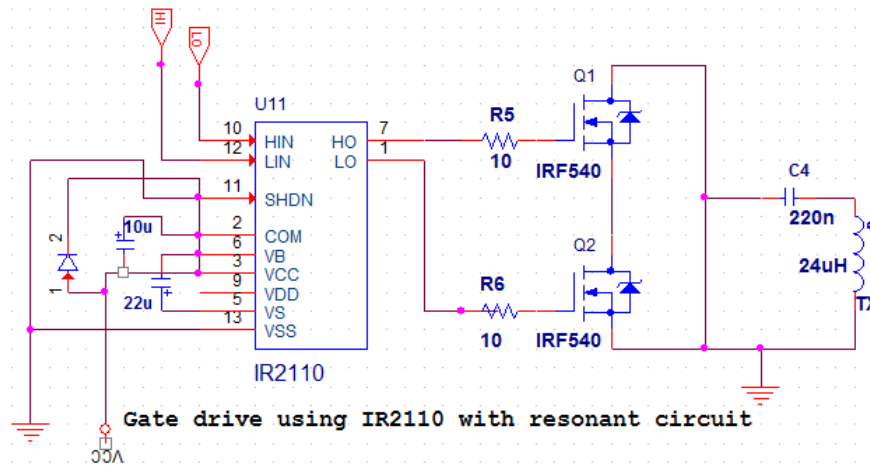


Figure 4: Gate drive using IR2110 with resonant circuit

Integrated circuit IR2110 is used as gate driver device and the implementation circuit diagram with the resonant tank is shown in figure 4. IR2110 is high voltage, high speed power MOSFET and IGBT drivers with independent high and low side referenced output channels. It features include floating channel designed for bootstrap operation between 500 V or 600V, gate drive supply output voltage ranging between 10 – 20 V, Matched propagation delay for both channels and outputs in phase with input. In order to obtain the high side voltage gate signal an external bootstrap capacitor and diode will be needed for this design. The bootstrap capacitor, C_{BST} is the most important component in the gate drive circuit; because it has to filter the high peak current charging the gate of the main MOSFET while providing bias for the source referenced floating circuitry. In every switching cycle during normal operation of the MOSFET, the bootstrap capacitor provides the total gate charge (Q_G) to turn-on the MOSFET, the reverse recovery charge (Q_{RR}) and leakage current of the bootstrap diode ($I_{L,K,D}$), the quiescent current of the level shifter ($I_{Q,LS}$) and the gate driver ($I_{Q,DRV}$), and the leakage current between the gate-source terminals (I_{GS}), including the current drawn by a potential gate to- source pull down

resistor. It should be noted that some of these currents flow only during the on-time of the MOSFET and some are actually zero depending on the implementation of the driver [5].

An approach in calculating bootstrap capacitor is to know the MOSFET that will be used for this design. IRF540NPbF HEXFET® Power MOSFET is choosing for this design. The benefit of this device is to achieve extremely low on-resistance per silicon area that leads to extremely efficient and reliable device for use in a wide variety of applications. From the data sheet of this device the total gate charge (Q_{gtot}) is 71 nC and gate – source voltage of 10V in order to ensure that the drain current is 16A [6]. It should be noted here that, the circuit operates at switching frequency of 100 kHz and operated between 500 – 600V as stated in the datasheet. The bootstrap capacitor is designed such that it can hold enough charge to prevent the voltage supply from dropping below either the MOSFET threshold voltage ranging between 2 – 4V or the gate – source voltage of 10V. The period of oscillation when the gate charge pulse of 71nC occurs

$$T_{sw} = \frac{1}{f_{sw}} = \frac{1}{100000} = 10\mu s$$

When 12V is supply, the capacitor should be large enough to prevent this voltage dropping below the minimum operating voltage (i.e. 10V) across the on – time.

If the total gate charge (Q_{gtot}) = total charge of bootstrap capacitor

$$Q_{gtot} = Q_{CB} = C_B dV [7]$$

Where C_B is the bootstrap capacitor and $\Delta V = \text{undervoltage} - \text{lockout}$

For a full charge value $\Delta V = 12 - 10 = 2V$

$$C_{B(min)} = \frac{Q_{gtot}}{2} = \frac{71 \times 10^{-9}}{2} = 35.5nF$$

It is good practice to ensure that the gate charge required is at least 10 times less from the charge capable of being supplied from the bootstrap capacitor before the voltage across it drops below the minimum supply, in this case the $C_{B(min)}$ is multiply by 10 [7].

$$C_{B(min)} = 35.5 \times 10 = 355nF$$

The value 355 nF is absolute minimum bootstrap capacitor and in the design a value for this capacitor can be chosen above this value.

Also, average current by the capacitor charging diode in the circuit can be derive from

$$I = \frac{dQ}{dt} = I_{avg} = \frac{71 \times 10^{-9}}{100 \times 10^{-6}} = 0.71mA$$

Since, it involves two MOSFETs that is for high and low sides, the average current should be multiply by 2

$$I_{avg} = 0.71mA \times 2 = 1.43mA$$

So, the diode should be able to handle an average forward current of 1.43mA. For an IRF450 HEXFET power MOSFET operating at 100 kHz it is approximately 1.4 mA.

The reverse blocking voltage for the diode should be a maximum of $600 + 12 = 612V$. In order to obtain a reliable 600V diode will be used for this design. The duty cycle used in the implementation of gate drive circuit is $\delta = 0.5$

3.2.1 Resonant tank

In order to know the values for the capacitor and inductor need for resonant tank, there is need to calculate the estimated efficiency of whole converter, maximum and minimum voltage gain for the resonant network, assumed transformer turn ratio and load resistance for this topology and the values of these components are implemented in the circuit diagram (i.e. figure 4) that involved the gate drive and the resonant tank.

3.2.2 Estimated efficiency

The efficiency of this converter will be estimated based on the maximum input power and maximum output power. The efficiency will be calculated with this equation

$$Efficiency (E_{ff}) = \frac{P_{output}}{P_{input}}$$

Given Output current = 500 mA and the Output voltage = 5 Volts

$$P_{output} = I_{output} \times Output\ voltage$$

$$P_{output} = 500 \times 5 = 2.5W$$

Since there is no reference data for the efficiency, then $E_{ff} = 0.88 \sim 0.92$ [4] will be used for low voltage output for this power converter $E_{ff} = 0.88$

$$P_{input} = \frac{P_{output}}{Efficiency (E_{ff})} = \frac{2.5W}{0.88} = 2.8 W$$

So, the input power P_{input} is 2.8 W

3.2.3 Maximum and Minimum voltage gains of the resonant network

It is in order to operate the LLC resonant converter around the resonant frequency in normal operation to minimize switching frequency variation. The maximum input voltage is used in order to obtain the minimum gain at the resonant frequency using the following formula

$$M^{min} = \frac{K + 1}{K}$$

Where M^{min} is the minimum voltage gain and K is is the gain at resonant frequency obtained as a function between the magnetizing inductance and primary side leakage inductance. It should be noted that, the value of K is set between 5~10, then a small value of k may lead to poor coupling of transformer and poor efficiency [4]. Let $K = 9$,

$$M^{min} = \frac{9 + 1}{9} = 1.1$$

The minimum voltage gain is 1.1

M^{max} is the maximum voltage gain and this can be obtain by using

$$M^{max} = \frac{V_{in}^{max}}{V_{in}^{min}} M^{min} = \frac{32 \times 1.1}{16} = 2.2$$

The maximum voltage gain is 2.2.

3.3.4 The Transformer Turns Ratio

In the proposed Half-Bridge LLC resonant converter, the full wave bridge rectifier will be used then, the transformer turns ratio is given by this formula

$$n = \frac{N_p}{N_s} = \frac{V_{in}^{max}}{(V_{out} + 2V_F)} M^{min}$$

It should be noted that a little modification will be made on the circuit which will be shown later on this work then n becomes

$$n = \frac{N_p}{N_s} = \frac{V_{in}^{max}}{2V_{out}} M^{min} = \frac{32}{2 \times 5} \times 1.1 = 3.52$$

The transformer turns ratio for the resonant converter is approximately equal to 4.

3.3.5 Load Resistance

The equivalent load resistance when the transformer turns ratio is 4, then

$$R_{ac} = \frac{8n^2 \times V_o^2 \times E_{ff}}{\pi^2 \times P_o} = \frac{8(4)^2(5)^2(0.88)}{(3.142)^2(2.5)} = 98 \Omega$$

The calculated load resistance is 98Ω.

3.3.6 The Resonant Network

Deduce from the Gain curve, the value of resonant frequency is 105 KHz but the trade off 10% is observed and make the actual resonant frequency to be 100 KHz.

Q = 10% of Maximum voltage gain + Maximum voltage gain [4]

$$Q = 0.22 + 2.2 = 2.42$$

The resonant components are resonant capacitor C_r , resonant inductor L_r and magnetic inductor, L_m

The resonant capacitor will be calculated using this expression below

$$C_r = \frac{1}{2\pi \times Q \times f_o \times R_{ac}} = \frac{1}{2 \times 3.142 \times 0.25 \times 100 \times 10^3 \times 98} = 64nF$$

The resonant inductor will be known using the expression

$$L_r = \frac{1}{(2\pi f_o)^2 \times C_r} = \frac{1}{(2\pi \times 100 \times 10^3)^2 \times 64 \times 10^{-9}} = 40\mu H$$

The magnetizing inductor will also be known from the expression below

$$L_m = \frac{(k + 1)^2 \times L_r}{(2k + 1)} = \frac{(9 + 1)^2 \times 40 \times 10^{-6}}{(2 \times 9 + 1)} = 211\mu H$$

The resonant capacitor, resonant inductor and magnetizing inductor are 64nF, 40μH and 211μH respectively. These values will be used for simulation and real circuit construction.

3.3.7 Current and Voltage Rating

In this design a current rating and voltage should be put into consideration for the resonant capacitor as the considerable amount of current is flowing through it. The root mean square current through resonant capacitor is given as

$$I_{C_r}^{RMS} = \sqrt{\left(\frac{\pi I_0}{2\sqrt{2}n}\right)^2 + \left(\frac{n(V_0+2V_f)}{4\sqrt{2}f_0 L_m}\right)^2} = \sqrt{\left(\frac{\pi \times 0.5}{2\sqrt{2} \times 4}\right)^2 + \left(\frac{4(5)}{4\sqrt{2} \times 100 \times 10^3 \times 221 \times 10^{-6}}\right)^2} = 0.211A$$

$$V_{C_r}^{Max} \cong \frac{V_{in}^{max}}{2} + \frac{\sqrt{2} \times I_{C_r}^{RMS}}{2\pi f_0 C_r} \cong \frac{36}{2} + \frac{\sqrt{2} \times 0.211}{2\pi \times 100 \times 10^3 \times 64 \times 10^{-9}} \cong 25 V$$

The maximum voltage of the resonant capacitor, when it is in operation is 25 V

3.4 RECEIVER CIRCUIT

The receiver circuit of this charging system is consist of the receiver charging coil, the bridge rectifier that consist of four diodes that rectify the alternating signal to direct current, the capacitors for holding and smoothing the pulsating direct current generated, the voltage regulator and the load resistor for the testing of output voltage as shown in figure 5. The choosing of the components for this circuit such as capacitors, diodes, voltage regulator and load resistor are based upon the simulation using LTSpice IV which will shown in the later part of this report.

This circuit operates based on the diodes and the signal received from the receiver coil. The diode D₁ and D₄ are forward biased when the AC signal received from the receiver coil is positive. During the negative cycle of the AC signal from the coil D₂ and D₃ are forward biased which maintain a positive voltage at the output. The output is passing through the capacitor to the voltage regulator and another capacitor for the smoothing of the output voltage.

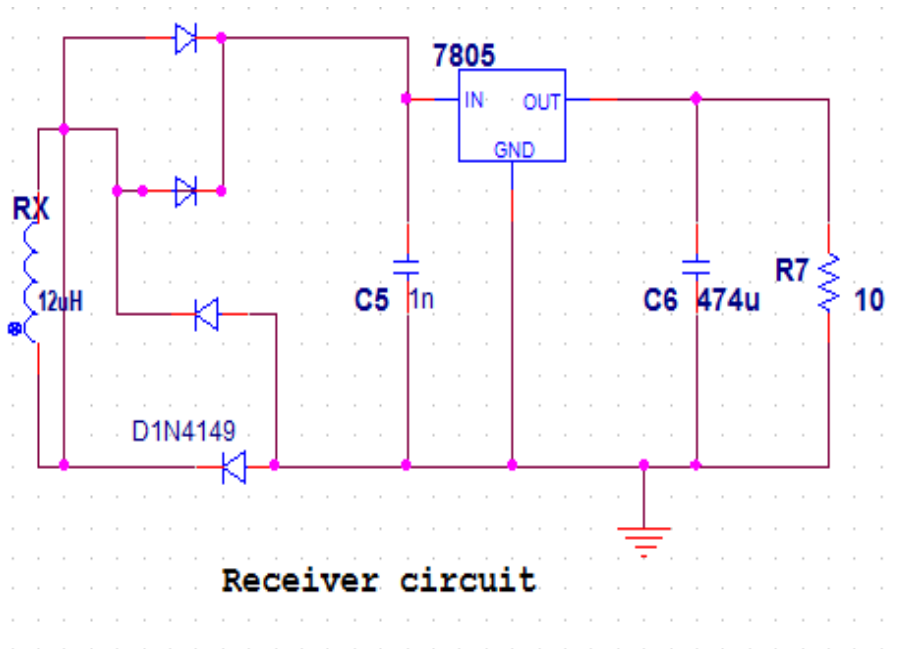


Figure 5: Receiver circuit

4.0 Implementation

In order to implement the Non-contact charging system circuit, steps are taken to ensure that each module (i.e. Pulse Width Modulation circuit, Gate drive circuit and the receiver circuit) are well connected and functioning properly. These modules were first placed on the breadboard after one another to ensure that the components have proper connection and functionality and to avoid short circuit that can cause problem for the entire design.

The first module to be constructed is the Pulse Width Modulation circuit as shown in figure 3, this is done by first placed the integrated circuit (TL494) on the breadboard followed by connecting the wires one going to grounds and Vcc, other passive components such as resistors and capacitor after which there values are known respectively. After all the connections, this module is tested and the result obtained in term of voltage and waveform on Pin 5, 9 and 10 of the chip is been reported on the later part of this report.

The second module is the gate drive circuit as shown in figure 4, the integrated circuit (IR2110) is placed on the breadboard followed by connecting all the components such as diode, resistors and capacitors and the wires going to the ground and Vcc. The output on the chip is connected to the two MOSFETs respectively. The resonant capacitor and the charging coil for the transmission were also connected respectively. In order to test this circuit, the connections were made to respective pins on the MOSFETs as the output on pin 1 and 7 were measured and recorded in term of voltage and waveform.

The third module is the receiver circuit shown in figure 5, the bridge rectifier diode was placed, while other components such as capacitors, resistor, LED as an indicator and load resistor were all connected with charging coil (i.e. receiver coil). This circuit was also tested and results in term of the voltage and waveform were reported respectively.

Having satisfies with the connections of the modules on the breadboard; all the components were carefully transferred and soldered on the strip board for the final testing.

5.0 Simulation and testing results

In this section, the results from the simulated circuit and implemented circuit are shown in term of the voltage and waveform. The complete circuit diagrams were shown in the Appendix A and B for both

simulation and implementation circuits. As stated in the implementation section, the control of this circuit was done by two main integrated circuits TL494 and IR2110. For the simulation LTSpice IV was used. Although, there is no provision for both TL494 and IR2110 in this simulation package and instead LTC 4444 was used for both PWM and gate drive circuits.

On the implementation circuit, 20 V was supplied to the circuit through Vcc as shown in Appendix A, on the Pulse Width Modulation circuit Pin 9 and 10, the voltage measured were 12.9 V respectively and the waveform is shown in figure 6.

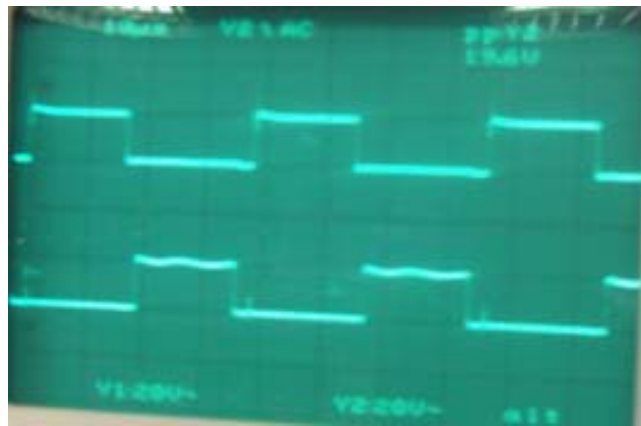


Figure 6: Waveform generated at Pin 9 and 10 of PWM circuit

From figure 6, the waveform generated in alternating mode of the circuit, which confirm the essence of using TL494 integrated circuit for the driving the gates of the MOSFETs.

On the gate drive circuit, the 12.9 V from Pin 9 and 10 of TL494 was supplied to Pin 10 (HIN) and 12 (LIN) of IR2110. While 13.1 V from Pin 1 (LO) and 25.8 V from Pin 7 (HO) were measured respectively from IR2110 and the waveform generated shown in figure 7A. These voltages measured from Pin 1 and 7 of IR2110 were fed into the gates of both MOSFETs Q1 and Q2 respectively.

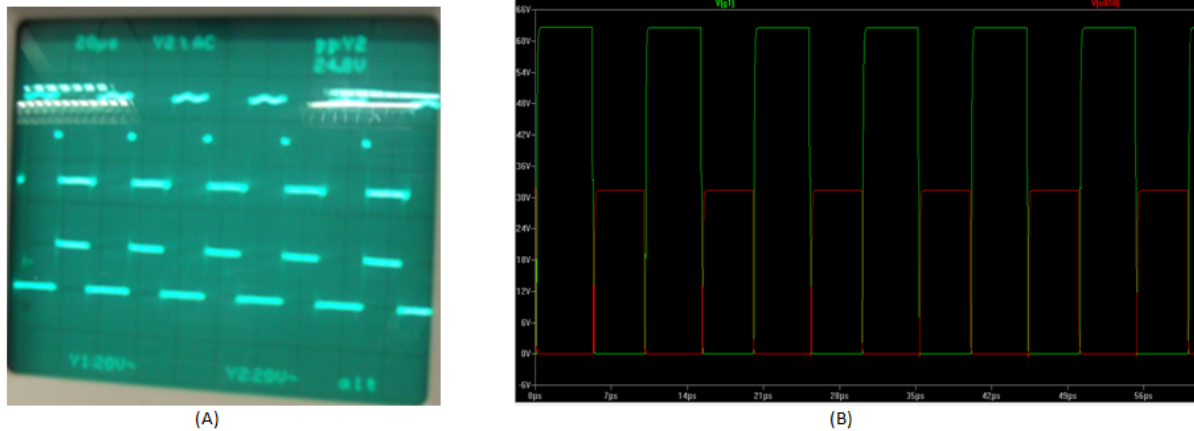


Figure 7: (A) Waveform generated from IR2110 and (B) Waveform generated for the gate drive from simulated circuit

Figure 7B, shows the simulated waveform generated by LTC 4444, serves as both the PWM and gate drive chip. In the simulation, 32 V was used as V_{cc} , which serves as the maximum voltage for the design and in which the output voltage supplied to both low side and high side of the MOSFETs were 32 and 64 V respectively. This waveform shows conformity with the one measured from the implemented circuit. From the TL494, 14 V was measured from Pin 5 (V_{DD}) which is supplied to the source-drain of both MOSFETs and waveform for this pulse signal is shown in figure 8A.

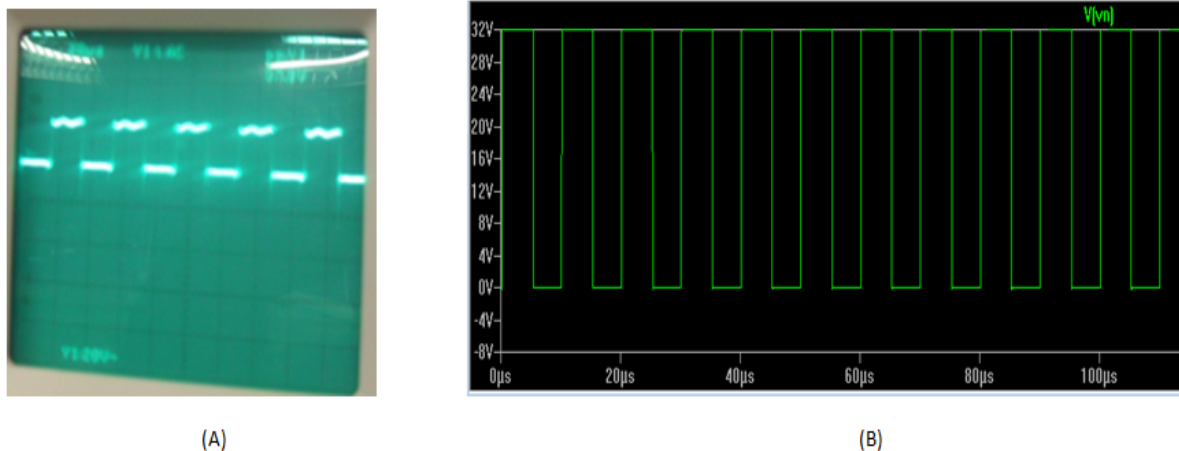


Figure 8: (A) Waveform generated from Pin 5 of TL494 and (B) Waveform generated from simulated circuit for V_{DS}

The waveform generated during the simulation shown in the figure 8B, which implies that there is correlation between the simulated and implemented circuit. It can be seen from figure 16, 32 V, was

supplied to the drain – source during the simulation, this high voltage is due to the voltage used for the simulation.

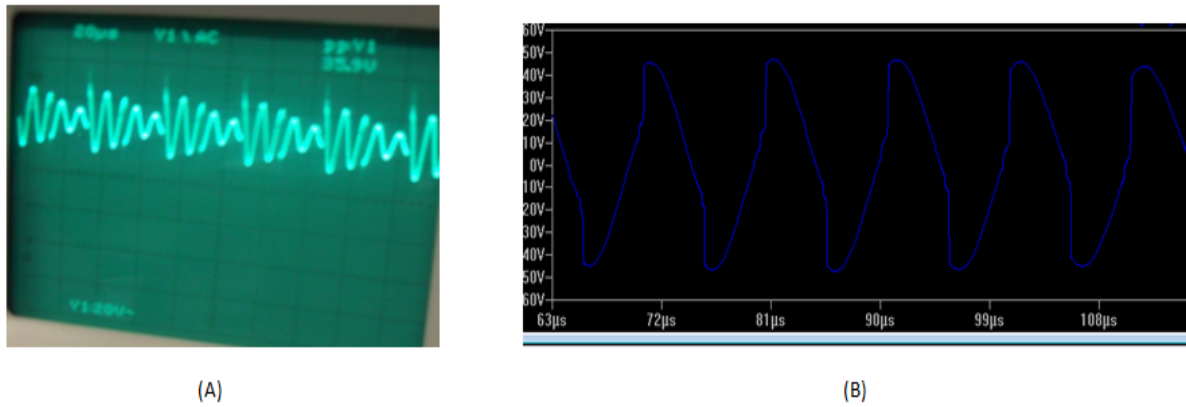


Figure 9: Resonant waveform generated from the implemented circuit and (B) Resonant waveform from simulated circuit

The figure 9A shows the sinusoidal waveform when the circuit is resonating, which serves as evidence for using this topology that is half bridge resonant converter. The importance of this sinusoidal signal generated is to be able to supply enough energy in the charging coil (transmitter) in order to transfer this energy to the receiver side of the circuit. Also shown in figure 9A, the resonating period of $10\mu\text{s}$ which is the same as 100 kHz as the confirmation for the frequency of the circuit. Figure 9B also shown the sinusoidal wave generated from the simulated circuit. It can be seen from figure 9 that, the waveform generated from the implemented and simulated circuits were almost the same.

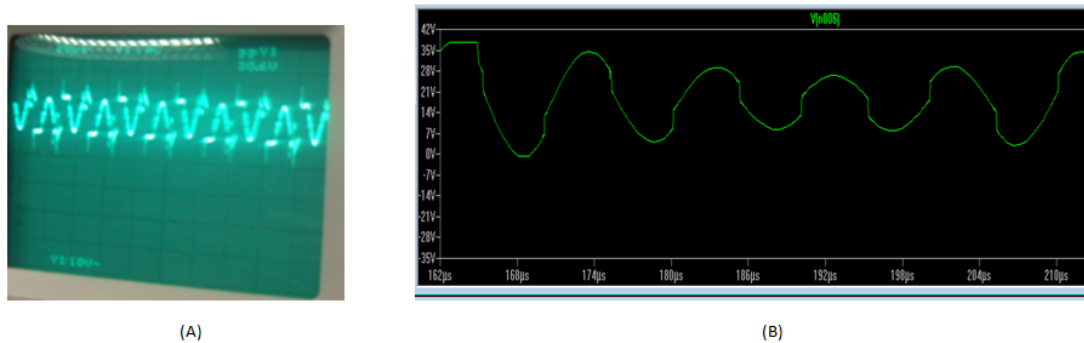
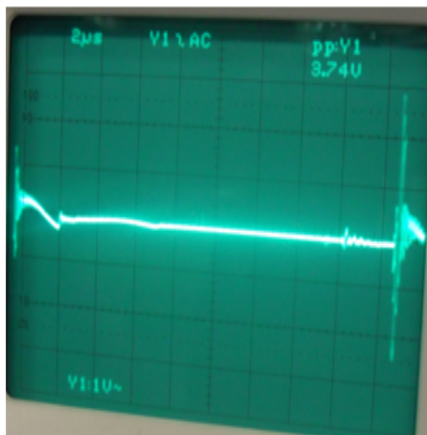


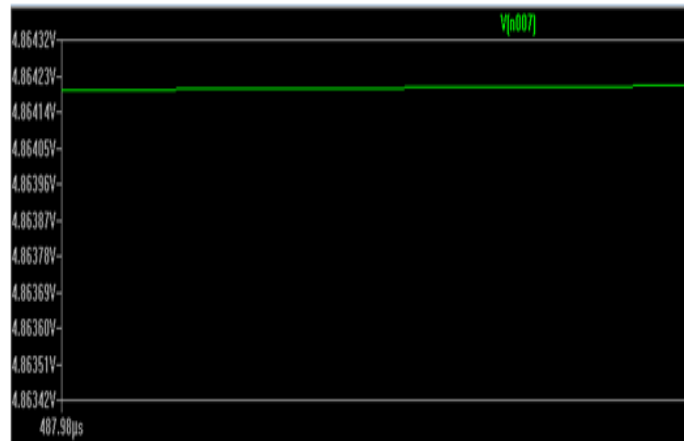
Figure 10: (A) Waveform generated after receiver coil in the circuit and (B) Waveform generated from simulated circuit after receiver coil

The waveform after receiver coil is shown in figure 10(A), which confirms the existences of resonant between the two coils. Even in figure 10 (B) of the simulated circuit, it shows that the waveform is not

perfect sinusoidal as correspond to the waveform generated in the implemented circuit shown in figure 10 (A). The voltages before and after the regulation was measured to be 6.2 and 5 V respectively from the implemented circuit. While the voltage, when there is load connected to the circuit is 3.1 V. The regulated waveforms were shown in figure 11 for both implemented and simulated circuits respectively.



(A)



(B)

Figure 11: (A) Regulated waveform generated in implemented circuit and (B) Regulated waveform from simulated circuit

In figure 11 (A), it can be seen that the waveform is not initially stable but after few micro seconds confirm some transient in the circuit which is inevitable as this is also observed in figure 11 (B) as presented in the regulated waveform of the simulated circuit.

From all the results obtained, there are much similarities between the waveforms obtained from both implemented and simulated circuit which indicate that the circuit is well constructed and properly placed on the strip board, but for the voltage measured, there are much disparity this due to the fact, 32 V is used for simulation while the power supply used for measurement in the laboratory is 20V in it maximum. Although, effort have been made to make the connections in series for the power in order to supply 32 V to the circuit for measurement.

6.0 Efficiency

It is not possible to determine the efficiency of the whole circuit but efficiency can be determine or calculated by ratio of the power absorbed by the receiver coil to the power consumed by the transmitting coil of the charging system.

$$\text{Efficiency} = \frac{\text{Voltage} \times \text{Current at the receiver coil}}{\text{Voltage} \times \text{Current at the transmission coil}} \times 100\%$$

The voltage measured at the receiver coil is 28 V and the current is 2A while the voltage measured at transmission coil is 30 V and 4 A respectively

$$\text{Efficiency} = \frac{28 \times 2}{30 \times 4} \times 100\% = 46\%$$

Although the efficiency calculated is 46% this can be attributed to some trade off that observed during the implementation of this design.

7.0 Conclusion

The design and implementation of Non-contact charging system for smartphones was successfully done. The success of this design is basically on understanding the theoretical operation of the chosen converter topology which half-bridge LLC resonant converter as the values for the components were calculated as the design was divided into three modules which are Pulse Width Modulation (PWM), gate driver and

the receiver. The specification given was partially meant as the voltage measured before and after the load were 5 V and 3.1 V respectively. The current of 25mA was achieved but low due to some trade off performed in the implementation of this design in order to operate within budget and the available power supply that cannot give more 20 V for the measurement. The operation principle of this design is basically inductive in which transmission coil transfer energy into receiver coil in order to achieve the objective of the design, as the efficiency between the coils was calculated to be 46 %. In order to generate control signals within the circuit designed TL494 integrated circuit was used at 50 % duty cycle for Pulse Width Modulation (PWM) while gate driver circuit was constructed with the uses of IR2110 in which the dead time between the two signals was also generated. The waveforms and voltage measured at each point of these integrated circuits were measured and reported as confirmation was established between the implemented and simulated circuits. This design is considered to be safe, simple, robust and cost efficient as against the conventional charging system which involves the connection of charger to the mains in order to charge smartphones.

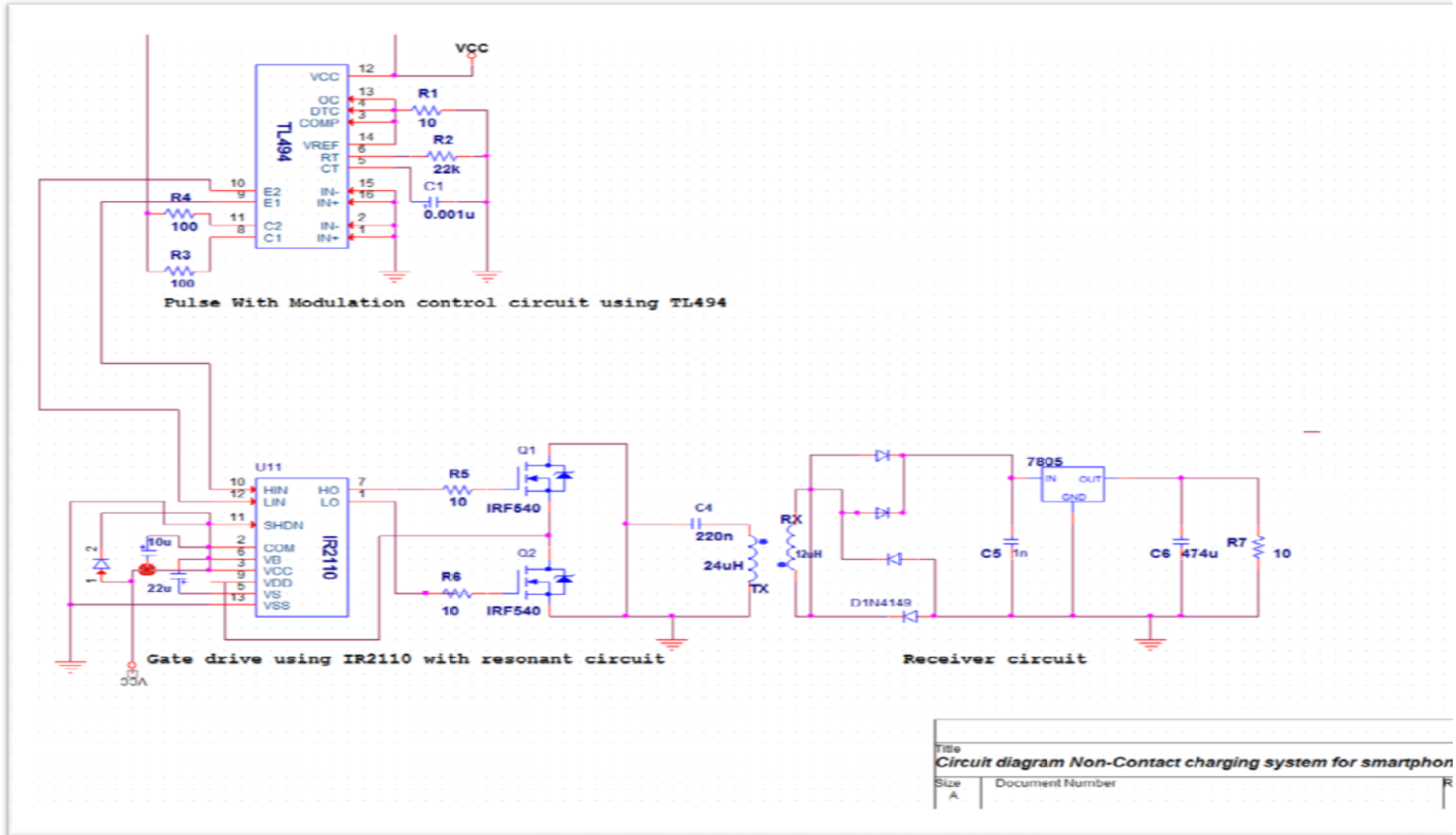
References

- [1] N. Carvalho, A. Costanzo, P. Mezzanotte, A. Soares and M. Pinuela, 'Wireless Power Transmission: R & D Activities Within Europe', *IEEE Transactions on Microwave Theory and Techniques*, vol 62, iss 4, p. 1, 2014.
- [2] G. Covic and J. Boys, 'Inductive power transfer', *IEEE*, 2013.
- [3] N. Chawla and S. Tosunoglu, 'State of the Art in Inductive Charging for Electronic Appliances and its Future in Transportation', *Florida conference on Recent Advances in Robotics*, p. 1, 2012.
- [4] U. Lockout, 'TL494, NCV494 SWITCHMODE™ Pulse Width Modulation Control Circuit', *Citeseer*, 2005.
- [5] L. Balogh, 'Design and application guide for high speed MOSFET gate drive circuits', 2001.
- [6] Data Sheet No. PD60147 data sheet for IR2110PBNF <http://www.irf.com/product-info/datasheets/data/ir2110.pdf>

Bibliography

- [1] M. Abdul Hamid, M. Seroji and M. Hidayat, 'Analysis Characteristics and Optimal Design Procedure of Half-Bridge LLC Loaded Resonant Converter', *IEEE International Conference on Power and Energy*, p. 2, 2012.
- [2] A. Sivaprasad, K. Deepa and K. Mathew, 'Half bridge Converter for Battery Charging Application', *International Journal of Engineering Research and Applications (IJERA)*, vol 2, iss 4, pp. 994-999, 2012.
- [3] K. Wang, C. Hsu, T. Chan, T. Chien and L. Chen, 'Study of applying contactless power transmission system to battery charge', pp. 257--262, 2009.
- [4] V. Sivachidambaranathan and S. Dash, 'Closed Loop Controlled LLC Half Bridge Isolated series Resonant Converter', *International Journal of Information and Electronics Engineering*, vol 1, iss 3, pp. 265-270, 2011.
- [6] Data sheet for TL494 http://www.onsemi.com/pub_link/Collateral/TL494-D.PDF
- [7] R. W. Erickson and D. Maksimovic, *Fundamentals of Power Electronics*. Springer; 2nd edition, 2001.
- [8] B. Mammano, *_Resonant mode converter topologies_*, pp. 1_2, 2001. Texas Instruments application note.
- [9] J.Gow Lecture note on Power electronics De Montfort University, Leicester, 2014

Appendix A



Appendix B

